Exploring the Surface Reactivity of 3d Metal Endofullerenes: A Density-Functional Theory Study

Rubén E. Estrada-Salas* and Ariel A. Valladares*

Departamento de Materia Condensada y Criogenia, Instituto de Investigaciones en Materiales, Universidad Nacional Autónoma de México, México D. F., C. P. 04510, México

Received: April 1, 2009; Revised Manuscript Received: August 4, 2009

Changes in the preferential sites of electrophilic, nucleophilic, and radical attacks on the pristine C_{60} surface with endohedral doping using 3d transition metal atoms were studied via two useful reactivity indices, namely the Fukui functions and the molecular electrostatic potential. Both of these were calculated at the density functional BPW91 level of theory with the DNP basis set. Our results clearly show changes in the preferential reactivity sites on the fullerene surface when it is doped with Mn, Fe, Co, or Ni atoms, whereas there are no significant changes in the preferential reactivity sites on the C_{60} surface upon endohedral doping with Cu and Zn atoms. Electron affinities (E_A), ionization potentials (I_P), and HOMO−LUMO gaps (E_g) were also calculated to complete the study of the endofullerene's surface reactivity. These findings provide insight into endofullerene functionalization, an important issue in their application.

1. Introduction

There has been an increasing interest in fullerenes endohedrally doped with late 3d transition metal atoms because they constitute a new class of unconventional endofullerenes[1] which may show paramagnetic behavior, since transition metal atoms commonly have unpaired spins in their 3d shell. For this reason, this new type of endofullerene could have potential applications in diverse fields ranging from magnetic resonance imaging (MRI) to spintronics and quantum computing.[2−6]

To the best of our knowledge, there are only a few reports on the synthesis (or attempts to synthesize) and characterization of unconventional endofullerenes with late 3d transition metal atoms (groups 7−12 of the Periodic Table).[1,7−18] However, recently, some companies have started to produce and commercialize some of these new endohedral metallofullerenes at very low costs,[15−19] making them attractive materials for experimental research and industrial applications. Theoretical studies have an important role to investigate the structural and electronic properties of this type of endofullerene and predict their striking characteristics.[20−31]

However, the chemical functionalization of endofullerenes is important in order to increase their water solubility (e.g., for MRI applications)[6] as well as to be able to handle them for fabrication of quantum computing or spintronic devices.[5]

In this work we study the surface reactivity of six 3d metal endofullerenes ($Mn@C_{60}$, $Fe@C_{60}$, $Co@C_{60}$, $Ni@C_{60}$, $Cu@C_{60}$, and $Zn@C_{60}$) by means of all-electron density-functional theory (DFT) calculations of their molecular electrostatic potentials (MEP) and their Fukui functions: two useful reactivity indices.[32] For a clear visualization of the endofullerenes surface reactivity, both the MEP and Fukui functions were mapped onto and isosurface of the total electron density of each endofullerene.

In order to predict a molecule's reactive behavior, a number of theoretical reactivity indices, obtainable from the electron density $\rho(r)$, are available. One of them is the frequently used molecular electrostatic potential (MEP), $\phi(r)$, defined as the interaction energy of the molecule with a positive test charge placed at position r:[32,33]

$$\phi(r) = \sum_A \frac{Z_A}{|r - r_A|} - \int \frac{\rho(r')}{|r - r'|} dr' \qquad (1)$$

where the summation runs over all the nuclei A in the molecule. Due to its definition, the MEP can readily be used in the study of electrophilic attacks and can be expected to describe mainly the hard−hard interactions between the reacting systems.[32] An electrophilic species will preferentially attack a molecule at sites where the MEP is most negative.[33]

The Fukui function, describing the soft−soft interactions between the reagents, is defined as follows:[32]

$$f(r) = \left[\frac{\delta\mu}{\delta\nu(r)}\right]_N = \left[\frac{\partial\rho(r)}{\partial N}\right]_\nu \qquad (2)$$

Because of the discontinuity in eq 2—the electron number N can change only by integer values—different physical meanings have been associated with the left and right derivatives as well as with their average value, corresponding to a reactivity index for an electrophilic attack [$f^-(r)$], a nucleophilic attack [$f^+(r)$], and a reactivity index for a radical attack [$f^0(r)$], respectively.[32,34]

In a previous work,[35] we performed full geometry optimization calculations for these six 3d metal endofullerenes considering five initial positions of the endoatom: (1) in the center of the cage, $M@C_{60}^c$; (2) on top of a hexagonal face, $M@C_{60}^h$; (3) on top of a pentagonal face, $M@C_{60}^p$; (4) on top of the bond shared by two hexagonal faces, $M@C_{60}^{h/h}$; and (5) on top of the bond shared by a pentagonal face and a hexagonal one, $M@C_{60}^{h/p}$.

The minimal energy structure of each endofullerene was obtained and confirmed by frequency analysis and ab initio molecular dynamics at room temperature: while in the minimal energy structure of $Mn@C_{60}$ and $Fe@C_{60}$, the endoatom is on top of a hexagonal face ($M@C_{60}^h$), in the minimal energy structure of $Cu@C_{60}$ and $Zn@C_{60}$ the endoatom is at the center of the C_{60} cage ($M@C_{60}^c$). The endofullerenes $Co@C_{60}$ and $Ni@C_{60}$ showed two minimal energy structures: one with the endoatom on top of a hexagonal face ($M@C_{60}^h$), and the other with the endoatom on top of a pentagonal face ($M@C_{60}^p$).

* To whom correspondence should be addressed. Tel./Fax: +52-55 5622 4636. E-mail: eduardo.estrada@correo.unam.mx, valladar@unam.mx.

10.1021/jp9029979 CCC: $40.75
Published on Web 08/26/2009

TABLE 1: Total Energies (E_T); Binding Energies (E_B); HOMO-LUMO Gaps (E_G); Vertical, Adiabatic and Experimental Electron Affinities ($^{V}E_A$, $^{A}E_A$, $^{Exp}E_A$, respectively); and Ionization Potentials ($^{V}I_P$, $^{A}I_P$, $^{Exp}I_P$, respectively)[a,b]

fullerene	total energy (E_T) [eV]	binding energy (E_B) [eV]	HOMO−LUMO gap (E_G) [eV] calc.	HOMO−LUMO gap (E_G) [eV] exp.	electron affinity [eV] $^{V}E_A$	electron affinity [eV] $^{A}E_A$	electron affinity [eV] $^{Exp}E_A$	ionization potential [eV] $^{V}I_P$	ionization potential [eV] $^{A}I_P$	ionization potential [eV] $^{Exp}I_P$
Mn@C_{60}^{h}	−93,548.218	441.274	0.138		3.025	2.808		6.241	6.144	
Fe@C_{60}^{h}	−96,616.497	442.922	0.845		2.867	2.894		6.588	6.447	
Co@C_{60}^{h}	−99,856.806	443.346	0.159		2.838	3.044		6.271	6.013	
Co@C_{60}^{p}	−99,856.554	443.093	0.666		3.113	3.289		6.524	6.253	
Ni@C_{60}^{h}	−103,274.007	443.624	0.785		2.892	3.018		6.477	6.359	
Ni@C_{60}^{p}	−103,274.133	443.749	1.078		2.931	3.001		6.648	6.565	
Cu@C_{60}^{c}	−106,871.802	441.274	0.588		2.933	3.042		6.783	6.787	
Zn@C_{60}^{c}	−110,651.437	441.119	1.594		2.975	2.995		6.991	6.995	
Pristine C_{60}	−62,225.413	441.564	1.674	1.70[a]	2.883	2.981	2.65 ± 0.05[b]	7.040	6.999	7.58 ± 0.02[b]

[a] From refs 45, 49, and 50. [b] From refs 45, 51, and 52.

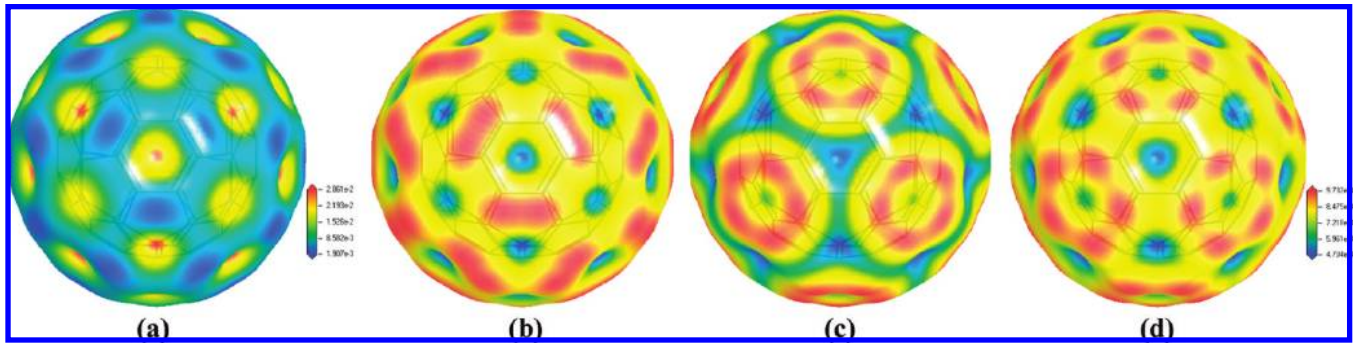

Figure 1. Pristine C_{60}: **(a)** MEP, **(b)** electrophilic, **(c)** nucleophilic, and **(d)** radical Fukui functions mapped onto an isosurface of the total electron density (isovalue = 0.017 au). For the Fukui functions, red zones show the highest susceptibility to attack, while blue zones show the lowest ones. For the MEP, red zones show its most positive value while blue zones show its most negative one. An electrophilic species will preferentially attack at sites where the MEP is most negative,[33] (blue).

Population analysis, molecular orbitals, electron density maps, HOMO−LUMO gaps (E_g), and binding energies (E_b) of these endofullerenes were also calculated in our previous work.[35]

2. Calculational Details

Total energy calculations were performed with the DFT-based program package *DMol*^{3}[36] at the generalized gradient approximation (GGA) density functional BPW91[37,38] level of theory with the double numerical atomic orbital basis set plus polarization functions (DNP). We chose the BPW91 functional because of its well tested good performance,[39−42] and also because the large dimension of the systems makes the use of higher order theoretical approaches such as the second-order many-body perturbation method (MP2) or the configuration interaction (CI) method, unfeasible.[43]

As pointed out above, for a clear visualization of the endofullerenes surface reactivity, both the MEP and Fukui functions were mapped onto an isosurface of the total electron density of each endofullerene. We also studied the pristine C_{60} surface reactivity in order to determine the changes in the preferential reactive sites through endohedral doping. We also calculated vertical and adiabatic electron affinities and ionization potentials for both endohedral and pristine C_{60} in order to complete the study of the endofullerenes surface reactivity.

The adiabatic ionization potential ($^{A}I_P$) refers to the formation of the molecular cation in its ground vibrational state and the vertical ionization potential ($^{V}I_P$) applies to the transition to the molecular cation without change in geometry.[44] However, the adiabatic electron affinity ($^{A}E_A$) is equal to the difference between the total energies of a neutral system and the corresponding anion, while the vertical electron affinity ($^{V}E_A$) is equal to the difference between total energies of a neutral system and the corresponding anion in the equilibrium geometry of the neutral system. VIPs and VEAs were calculated as the total energy difference between the optimized geometry of the neutral molecule and its corresponding one electron charged ions in the equilibrium geometry of the neutral molecule. Alternatively, AIPs and AEAs were calculated as the total energy difference between the optimized geometry of the neutral molecule and its corresponding one electron charged ions in its own optimized geometry.

3. Results and Discussion

It should be noted that after the subsection of endofullerenes stability, we present subsections in which we group, for the purpose of analysis, the endofullerenes according to the similarity of their chemical behavior; i.e., their reactivity.

3.1. Endofullerenes Stability. In Table 1, we report the total energies (E_T), binding energies (E_B), HOMO−LUMO gaps (E_G), electron affinities (E_A), and ionization potentials (I_P) of the endohedral metallofullerenes studied and of the pristine C_{60}. E_B is defined as the absolute value of the difference between the total energy of the molecule and the energy sum of the free atoms constituting the molecule, which is the usual standard for estimating the thermodynamic stability of a molecule.[25] Mn@C_{60}, Cu@C_{60}, and Zn@C_{60} molecules have an E_B lower than that of pristine C_{60}, whereas Fe@C_{60}, Co@C_{60} and Ni@C_{60} molecules have an E_B slightly higher than that of pristine C_{60}; however, all metallofullerenes seem to have almost the same stability as the pristine fullerene.

3.2. Reactivity of C_{60}, Zn@C_{60}, and Cu@C_{60}. In Figure 1 we can observe that for pristine C_{60}, both the MEP and the Fukui

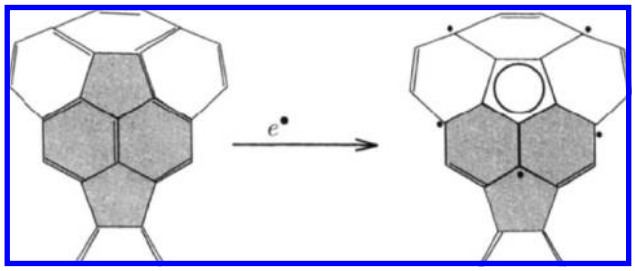

Figure 2. Addition of an electron to a pyracylene unit (shaded) of a fullerene to give an aromatic pentagonal ring.[45]

functions indicate that the highest susceptibility to electrophilic attack is on the double bonds shared by two hexagonal faces ([6,6]-bonds), in agreement with the experimental findings.[45−47] We can also observe for pristine C_{60} that the highest susceptibility for both nucleophilic and radical attack is on the single bonds shared by a hexagonal face and a pentagonal one ([5,6]-bonds), which is in good agreement with the experimental studies on C_{60} electrochemical reduction, where it has been proposed that the addition of electrons to the pentagonal rings is favored because it forms an aromatic cyclopentadienyl radical moiety, Figure 2.[45,48]

In Figure 3, we observe that the preferential sites for electrophilic, nucleophilic, and radical attacks remain practically unchanged despite the presence of the Zn endoatoms. This can be explained considering that there is practically no interaction between the Zn endoatom and C_{60}, which can be seen in both the absence of charge transfer from Zn to C_{60}, and the lack of orbital hybridization between the Zn and C_{60} orbitals, as was found in our previous work.[35] All of this agrees with the fact that the calculated values for the HOMO−LUMO gap, the electron affinity, and the ionization potential of $Zn@C_{60}^{c}$ are practically the same as those for pristine C_{60}, Table 1.

Figure 4 shows that the presence of the Cu endoatom practically does not affect the preferential sites for both nucleophilic and radical attacks with respect to pristine C_{60}. However, whereas the MEP shows no change in the preferential sites of electrophilic attack, Figure 4(a), the electrophilic Fukui function shows a significant decrease of the susceptibility to this attack on the [6,6]-bonds and a little increase on the [5,6]-bonds, Figure 4(b). This could be related to fact that the Cu endoatom have one unpaired electron (i.e., a free radical) localized in an energy level in the middle of the pristine C_{60} gap, Figure 5,[35] which causes a reduction of the HOMO−LUMO gap as well as a decrease in the ionization potential of the $Cu@C_{60}^{c}$ with respect to those of pristine C_{60}, table 1.

Consequently, the chemical behavior of the $Zn@C_{60}$ and $Cu@C_{60}$ will be practically the same than that of pristine C_{60}, so it is expected that the same kind and variety of reactions that occur in pristine C_{60} may take place in these two endofullerenes. This behavior has also been observed in other endofullerenes where the endoatom prefers to occupy the central position of the C_{60} cage, such as $N@C_{60}$ and $P@C_{60}$,[5,53] because they have all been functionalized with some of the same type of reactions used for pristine C_{60}.

3.3. Reactivity of $Mn@C_{60}$ and $Co@C_{60}$. The structures $Mn@C_{60}^{h}$ and $Co@C_{60}^{h}$ showed practically the same reactive behavior, Figure 6, against electrophilic, nucleophilic, and radical species, indicating an "amphoteric" behavior of these endofullerenes. The highest susceptibility to attack is on the face bonded to the endoatom.

The "amphoteric" behavior must be related to the fact that these two endofullerenes have semioccupied orbitals (Figure

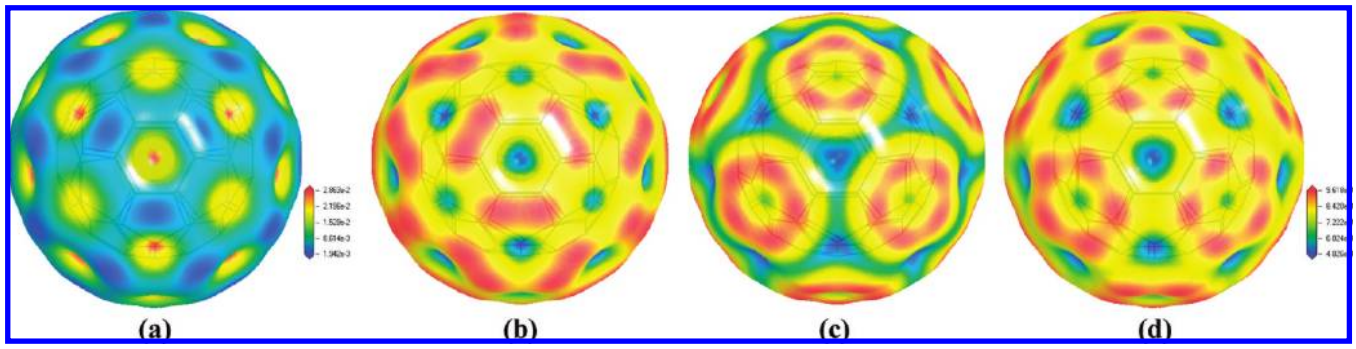

Figure 3. $Zn@C_{60}^{c}$: **(a)** MEP, **(b)** electrophilic, **(c)** nucleophilic, and **(d)** radical Fukui functions mapped onto an isosurface of the total electron density (isovalue = 0.017 au). The color code is the same as that for Figure 1.

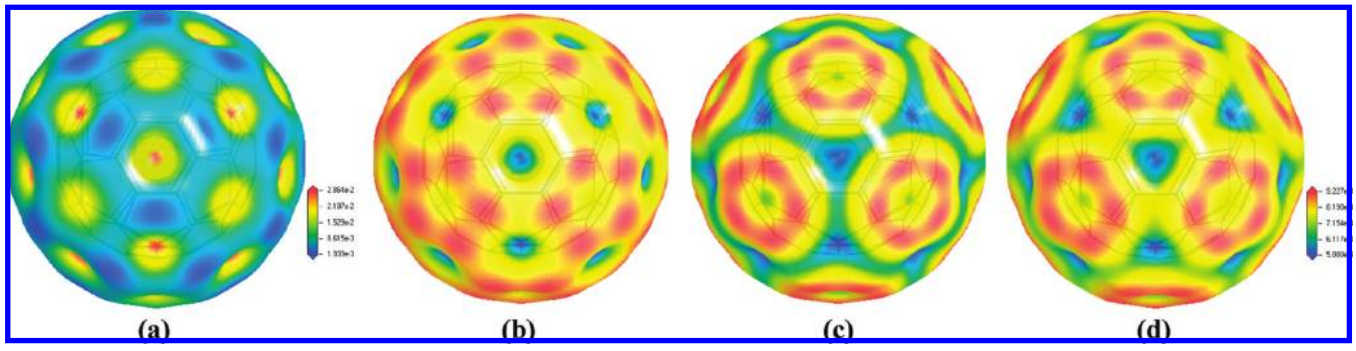

Figure 4. $Cu@C_{60}^{c}$: **(a)** MEP, **(b)** electrophilic, **(c)** nucleophilic, and **(d)** radical Fukui functions mapped onto an isosurface of the total electron density (isovalue = 0.017 au). The color code is the same as that for Figure 1.

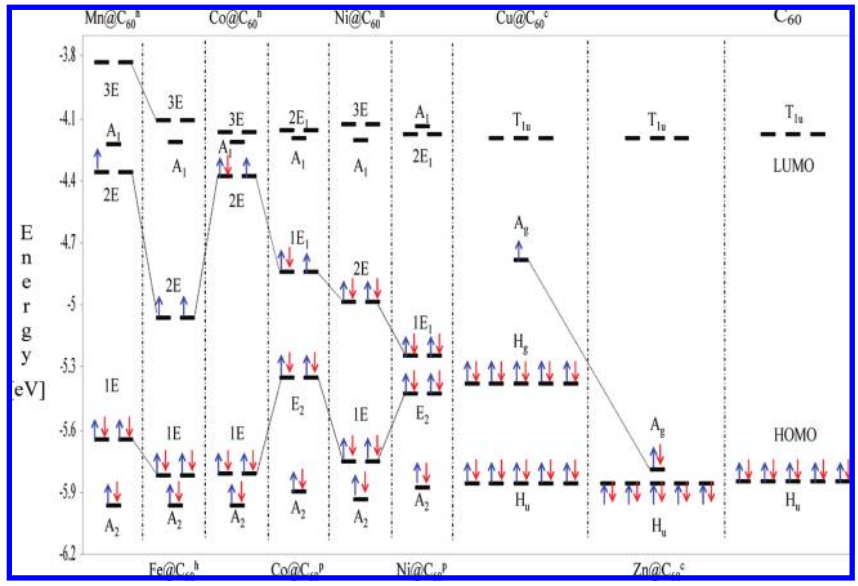

Figure 5. Kohn−Sham electronic levels of the six studied endohedral metallofullerenes and HOMO−LUMO levels of pristine C_{60}, as predicted at the BPW91/DNP level of theory. It should be mentioned that there exist differences between the up- and down-spin energies; however, these differences are not illustrated in this diagram for simplicity.[35]

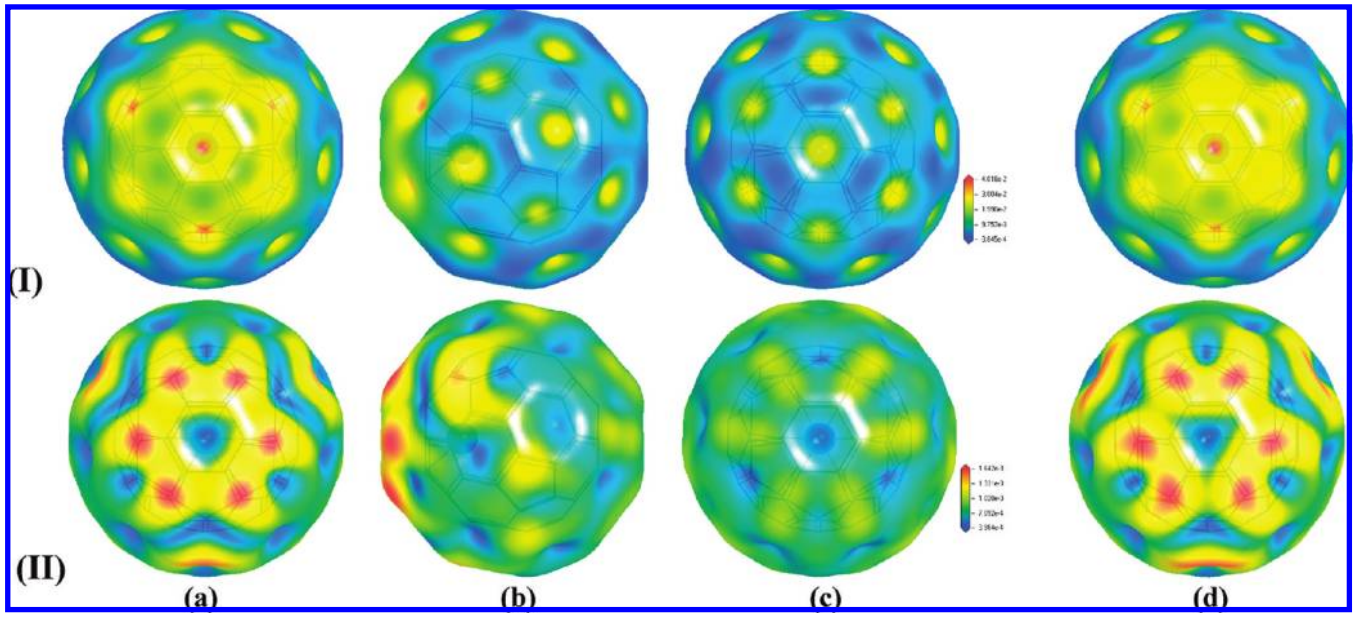

Figure 6. $Mn@C_{60}^{h}$: **(I)** MEP, and **(II)** electrophilic Fukui function mapped onto an isosurface of the total electron density (isovalue = 0.017 au): **(a)** Frontal view, **(b)** side view, and **(c)** rear view. We take as frontal view the hexagonal face bonded to the endoatom. The color code is the same as that for Figure 1. Nucleophilic and radical Fukui functions showed the same color mapping as the electrophilic one indicating an "amphoteric" behavior of $Mn@C_{60}^{h}$. **(d)** $Co@C_{60}^{h}$ showed practically the same color mapping as $Mn@C_{60}^{h}$ [See part **(a)**].

5) as well as HOMO−LUMO gaps quite small compared with that of pristine C_{60} (Table 1), so this allows them to have the ability to accept an electron in its semioccupied orbital as well as to donate this unpaired electron. This is because the energetic cost of any of these processes will be neither so high nor so low, considering the gaps value.

When the Co endoatom is on top of a pentagonal face ($Co@C_{60}^{p}$), the endofullerene still shows the "amphoteric" character against electrophilic, nucleophilic, and radical attacks, which also agrees with the fact that this endofullerene has a semioccupied orbital (Figure 5) as well as a HOMO−LUMO gap smaller than that of pristine C_{60} (Table 1).

In this conformation, the highest susceptibility to attack is located on the adjacent carbon atoms of the pentagonal face bonded to the Co or Mn endoatoms, Figure 7.

3.4. Reactivity of $Fe@C_{60}$ and $Ni@C_{60}$. The endofullerenes $Fe@C_{60}$ and $Ni@C_{60}$ do not show the "amphoteric" behavior presented by the endofullerenes $Mn@C_{60}$ and $Co@C_{60}$ against electrophilic, nucleophilic, and radical species.

For $Ni@C_{60}$, this is easy to understand since this endofullerene has no unpaired electrons, Figure 5. However, the lack of an "amphoteric" behavior in the case of $Fe@C_{60}$ is somewhat unexpected because this endofullerene has unpaired electrons as $Mn@C_{60}$ and $Co@C_{60}$.

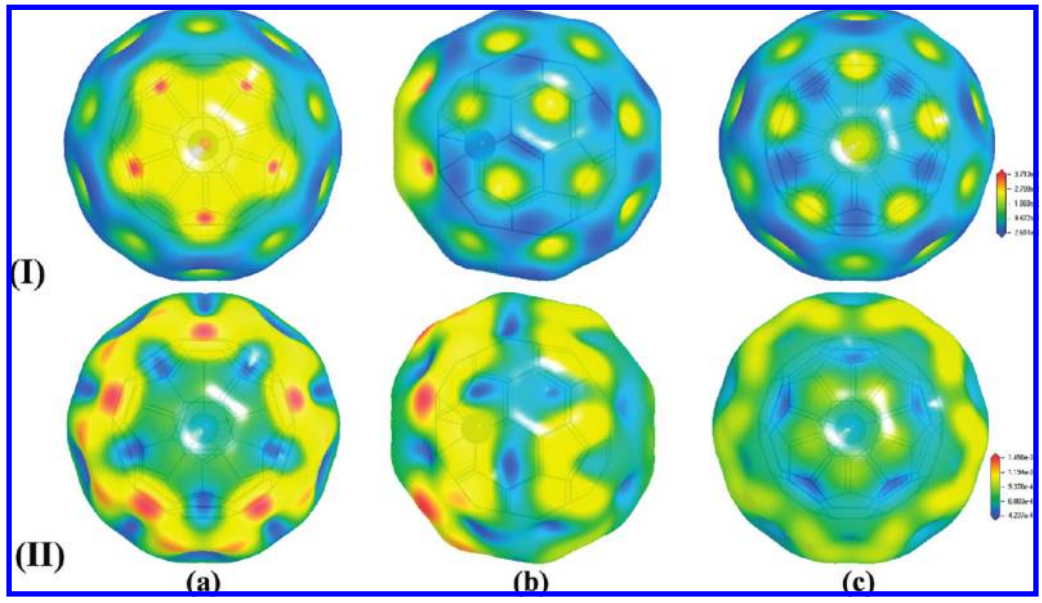

Figure 7. $Co@C_{60}^{p}$: **(I)** MEP, and **(II)** electrophilic Fukui function mapped onto an isosurface of the total electron density (isovalue = 0.017 au): **(a)** Frontal view, **(b)** side view, and **(c)** rear view. We take as frontal view the pentagonal face bonded to the endoatom. The color code is the same as that for Figure 1. Nucleophilic and radical Fukui functions showed the same color mapping as the electrophilic one indicating an "amphoteric" behavior of $Co@C_{60}^{p}$.

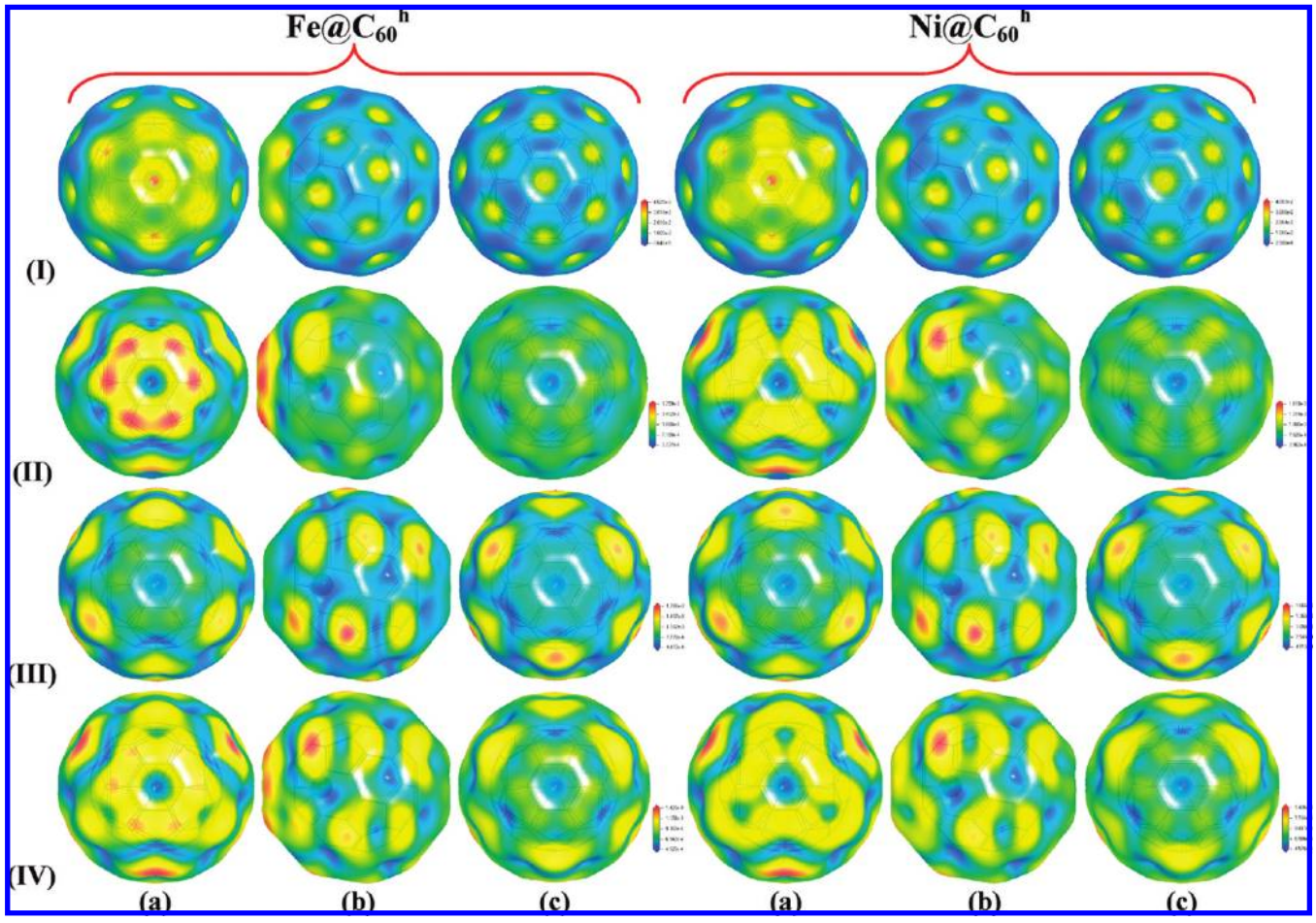

Figure 8. $Fe@C_{60}^{h}$ and $Ni@C_{60}^{h}$: **(I)** MEP, and **(II)** electrophilic, **(III)** nucleophilic, and **(IV)** radical Fukui functions mapped onto an isosurface of the total electron density (isovalue = 0.017 au): **(a)** Frontal view, **(b)** side view, and **(c)** rear view. We take as frontal view the hexagonal face bonded to the endoatom. The color code is the same as that for Figure 1.

In Figure 8, $Fe@C_{60}^{h}$ and $Ni@C_{60}^{h}$ are shown. The electrophilic Fukui function of the $Fe@C_{60}^{h}$ structure is broadly similar to that of the $Mn@C_{60}^{h}$ and $Co@C_{60}^{h}$ structures, reaching its highest susceptibility to attack on the face bonded to the endoatom. However, in the case of the $Ni@C_{60}^{h}$ structure the highest susceptibility to electrophilic attack is now on the fragments of

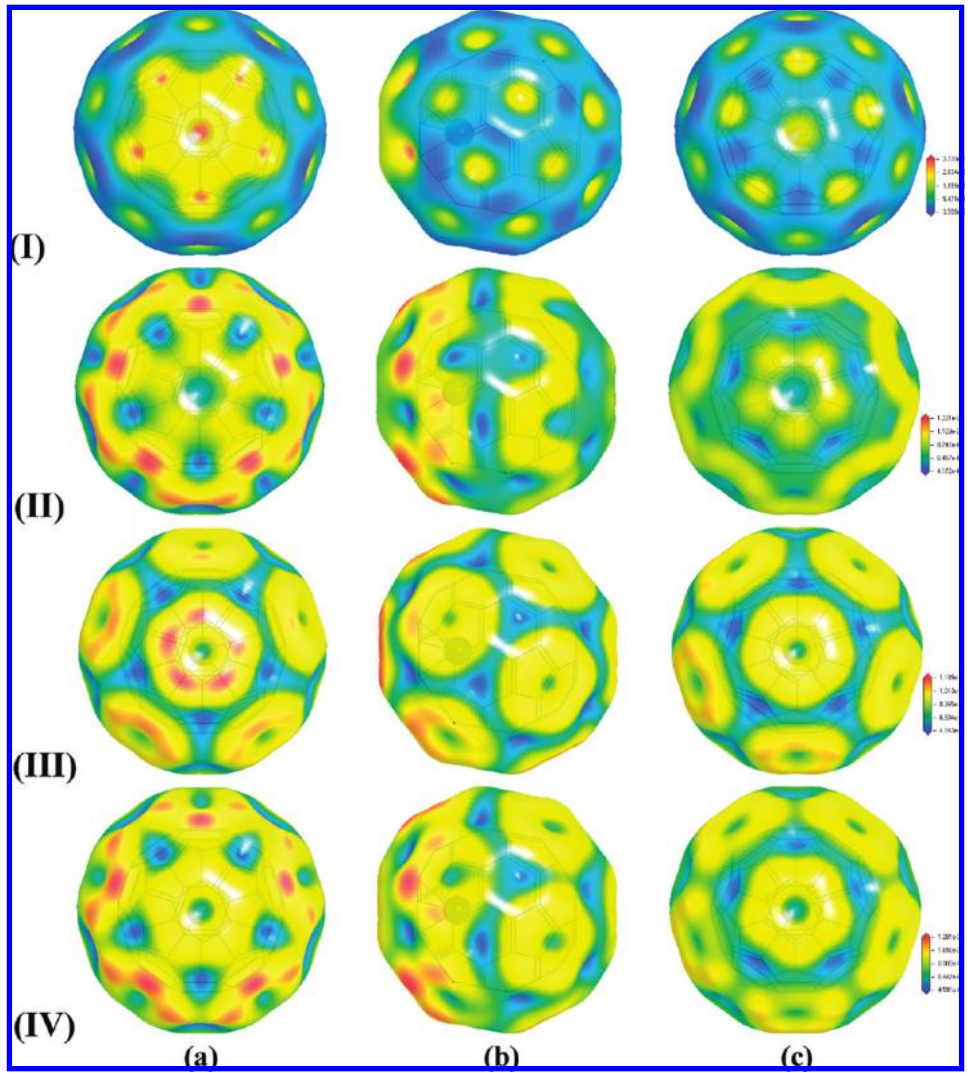

Figure 9. Ni@C_{60}^{p}: **(I)** MEP, and **(II)** electrophilic, **(III)** nucleophilic, and **(IV)** radical Fukui functions mapped onto an isosurface of the total electron density (isovalue = 0.017 au): **(a)** Frontal view, **(b)** side view, and **(c)** rear view. We take as frontal view the pentagonal face bonded to the endoatom. The color code is the same as for Figure 1.

the pentagonal faces which are adjacent to the face bonded to the endoatom.

The nucleophilic Fukui functions of the Fe@C_{60}^{h} and Ni@C_{60}^{h} structures are practically the same and both present a different color mapping from the Mn@C_{60}^{h} and Co@C_{60}^{h} structures.

The Ni@C_{60}^{p} conformation, Figure 9, does not show the "amphoteric" behavior presented by the Co@C_{60}^{p} structure, Figure 7.

4. Conclusions

In general, we can conclude that an endofullerene whose minimal energy structure is one that has the endoatom located at the center of the C_{60} cage (M@C_{60}^{c}), will show essentially the same chemical behavior as pure C_{60}. While an endofullerene whose minimal energy structure is one that has the endoatom located outside the center of the C_{60} cage (M@C_{60}^{h} or M@C_{60}^{p}) will show a markedly different chemical behavior as pristine C_{60}.

All of this indicates that whereas the Mn@C_{60} and Co@C_{60} endofullerenes could be functionalized by any kind of reagent (electrophile, nucleophile, or radical) at the same surface sites, the Fe@C_{60} and Ni@C_{60} will be functionalized at different surface sites depending on the kind of reagent (electrophile, nucleophile, or radical).

Acknowledgment. R.E.E.S. acknowledges the financial support of CONACyT during his Ph.D. studies. A.A.V. is grateful to DGAPA-UNAM for the funding of his scientific projects. Some of the calculations were carried out in the Computing Center of DGSCA-UNAM. Several comments by D. Díaz have been instrumental throughout this work. M.T. Vázquez has provided the information requested.

Supporting Information Available: This material is available free of charge via the Internet at http://pubs.acs.org.

References and Notes

(1) Huang, H.; Ata, M.; Yoshimoto, Y. *Chem. Commun.* **2004**, *2004*, 1206.
(2) Guha, S.; Nakamoto, K. *Coord. Chem. Rev.* **2005**, *249*, 1111.
(3) Shinohara, H. *Rep. Prog. Phys.* **2000**, *63*, 843.
(4) Liu, S.; Sun, S. *J. Organomet. Chem.* **2000**, *599*, 74.
(5) Harneit, W. *Phys. Rev. A* **2002**, *65*, 032322−1.
(6) Bolskar, R.; Benedetto, A.; Husebo, L.; Price, R.; Jackson, E.; Wallace, S.; Wilson, L.; Alford, J. *J. Am. Chem. Soc.* **2003**, *125*, 5471.
(7) Knapp, C.; Weiden, N.; Dinse, K. *Magn. Reson. Chem.* **2005**, *43*, S199.

(8) Elliot, B.; Yang, K.; Rao, A.; Arman, H.; Pennington, W.; Echegoyen, L. *Chem. Commun.* **2007**, *2007*, 2083.
(9) Basir, Y.; Anderson, S. *Chem. Phys. Lett.* **1995**, *243*, 45.
(10) Basir, Y.; Anderson, S. *Int. J. Mass Spectrom.* **1999**, *185/186/187*, 603.
(11) Pradeep, T.; Kulkarrii, G.; Kannan, K.; Guru Row, T.; Rao, C. N. R. *J. Am. Chem. Soc.* **1992**, *114*, 2272.
(12) Byszewski, P.; Kowalska, E.; Diduszko, R. *J. Therm. Anal.* **1995**, *45*, 1205.
(13) Churilov, G.; Bayukov, O.; Petrakovskaya, E.; Korets, A.; Isakova, V.; Titarenko, Y. N. *Tech. Phys.* **1997**, *42*, 1111.
(14) Reinke, P.; Eyhusen, S.; Büttner, M.; Oelhafen, P. *Appl. Phys. Lett.* **2004**, *84*, 4373.
(15) Edwards, C.; Butler, I.; Qian, W.; Rubin, Y. *J. Mol. Struct.* **1998**, *442*, 169.
(16) Avramov-Ivic, M.; Matija, L.; Antonovic, D.; Loutfy, R.; Lowe, T.; Rakin, P.; Koruga, D. *Trends Adv. Mater. Process. Mater. Sci. Forum* **2000**, *352*, 135.
(17) Ivetic, M.; Mojovic, Z.; Matija, L. *Stud. Adv. Mater. Process. Mater. Sci. Forum* **2003**, *413*, 49.
(18) Matija, L.; Avramov-Ivic, M.; Kapetanovic, V. *Contemp. Stud. Adv. Mater. Process. Mater. Sci. Forum* **2003**, *413*, 53.
(19) (a) Job, R. Solid Metal-Carbon Matrix of Metallofullerites and Method of Forming Same. U.S. Patent 5 288 342, 1994. (b) http://www.nsti.org/press/PRshow.html?id=1508. (c) http://www.jenlaurltd.com.
(20) Chang, A.; Ermler, W.; Pitzer, R. *J. Chem. Phys.* **1991**, *94*, 5004.
(21) Li, G.; Sabirianov, R.; Lu, J.; Zeng, X.; Mei, W. *J. Chem. Phys.* **2008**, *128*, 074304.
(22) Lu, J.; Ge, L.; Zhang, X.; Zhao, X. *Mod. Phys. Lett.* **1999**, *13*, 97.
(23) Gorelik, E.; Plakhutin, B. *J. Struct. Chem.* **2005**, *46*, 771.
(24) Kowalska, E.; Byszewski, P.; Dluzewski, P.; Diduszko, R.; Kucharski, Z. *J. Alloys Comp.* **1999**, *286*, 297.
(25) Tang, C.; Deng, K.; Yang, J.; Wang, X.; Chinese, J. *Chem.* **2006**, *24*, 1133.
(26) (a) Maruyama, S. FT-ICR Reaction Experiments and Molecular Dynamics Simulations of Precursor Clusters For SWNTs. in *Perspective of Fullerene Nanotechnology Part III*; Osawa, E., Ed.; Kluwer Academic Publisher: UK, 2002; pp 131, 142. (b) Yamaguchi, Y.; Maruyama, S. *Eur. Phys. J. D* **1999**, *9*, 385.
(27) Alemany, M.; Diéguez, O.; Rey, C.; Gallego, L. *J. Chem. Phys.* **2001**, *114*, 9371.
(28) Matija, L. *Arch. Oncol.* **1997**, *5*, 151.
(29) Shiga, K.; Ohno, K.; Maruyama, Y.; Kawazoe, Y.; Ohtsuki, T. *Modelling Simul. Mater. Sci. Eng.* **1999**, *7*, 621.
(30) Gurin, V. *Int. J. Quantum Chem.* **2005**, *104*, 249.
(31) Varganov, S.; Avramov, P.; Ovchinnikov, S. *J. Struct. Chem.* **2000**, *41*, 687.
(32) De Proft, F.; Martin, J.; Geerlings, P. *Chem. Phys. Lett.* **1996**, *256*, 400.
(33) Levine, I. *Quantum Chemistry* ,5th ed; Prentice Hall: NJ, 2000.
(34) Parr, R.; Yang, W. *Density-Functional Theory of Atoms and Molecules*; Oxford University Press: New York, 1989.
(35) Estrada-Salas, R.; Valladares, A. *J. Mol. Struct.: Theochem.* **2008**, *869*, 1.
(36) (a) Delley, B. *J. Chem. Phys.* **1990**, *92*, 508. (b) Delley, B. *J. Chem. Phys.* **2000**, *113*, 7756.
(37) Becke, A. *Phys. Rev. A* **1988**, *38*, 3098.
(38) Perdew, J.; Wang, Y. *Phys. Rev. B* **1992**, *45*, 13244.
(39) Koch, W.; Holthausen, M. *A Chemist's Guide to Density Functional Theory*; Wiley-VCH: Weinheim, 2001.
(40) Marlo, M.; Milman, V. *Phys. Rev. B* **2000**, *62*, 2899.
(41) Tsuzuki, S.; Lüthi, H. *J. Chem. Phys.* **2001**, *114*, 3949.
(42) Filatov, M.; Cremer, D. *J. Chem. Phys.* **2005**, *123*, 124101.
(43) Panavello, M.; Jalbout, A.; Trzaskowski, B.; Adamowicz, L. *Chem. Phys. Lett.* **2007**, *442*, 339.
(44) McNaught, A.; Wilkinson, A. *IUPAC Compendium of Chemical Terminology: The Gold Book*, 2nd ed. Blackwell Science: Cambridge, 1997.
(45) Dresselhaus, M.; Dresselhaus, G.; Eklund, P.; *Science of Fullerenes and Carbon Nanotubes*. 1996, Academic Press, San Diego.
(46) Kadish, K.; Ruoff, R. *Fullerenes: Chemistry, Physics, and Technology*; John Wiley & Sons: New York, 2000.
(47) (a) Taylor, R.; Walton, D. *Nature* **1993**, *363*, 685. (b) Taylor, R. *The Chemistry of Fullerenes*; World Scientific Publishing: Singapore 1995.
(48) Iikura, H.; Mori, H.; Sawamura, H.; Nakamura, E. *J. Org. Chem.* **1997**, *62*, 7912.
(49) Alemany, M.; Diéguez, O.; Rey, C.; Gallego, L. *J. Chem. Phys.* **2001**, *114*, 9371.
(50) Haufler, R.; Wang, L.; Chibante, L.; Jin, C.; Conceicao, J.; Chai, Y.; Smalley, R. *Chem. Phys. Lett.* **1991**, *179*, 449.
(51) Lichtenberger, D.; Nebesny, K.; Ray, C.; Huffman, D.; Lamb, L. *Chem. Phys. Lett.* **1991**, *176*, 203.
(52) de Vries, J.; Steger, H.; Kamke, B.; Menzel, C.; Weisser, B.; Kamke, W.; Hertel, I. *Chem. Phys. Lett.* **1992**, *188*, 159.
(53) Benjamin, S.; Ardavan, A.; Briggs, G.; Britz, D.; Gunlycke, D.; Jefferson, J.; Jones, M.; Leigh, D.; Lovett, B.; Khlobystov, A.; Lyon, S.; Morton, J.; Porfyrakis, K.; Sambrook, M.; Tyryshkin, A. *J. Phys.: Condens. Matter* **2006**, *18*, S867.

JP9029979